Experimental Investigations on Aerodynamic Response of Panel Structures at High Subsonic and Low Supersonic Mach Numbers.

Jannis Lübker
DLR, German Aerospace Center
PHD Student, Institut of Aeroelasticity
Bunsenstraße 10, 37073, Göttingen, Germany
Jannis.Luebker@dlr.de

Marko Alder
DLR, German Aerospace Center
PHD Student, Institut of Aerodynamics and Flow Technology
36108, Braunschweig, Germany

ABSTRACT

The phenomenon panel flutter is known since the mid 1940's. Intense investigations in experiment and theory followed in the 60's and 70's. The developed theories are capable of describing panel flutter in the subsonic and high supersonic Mach number domain but are insufficient in the transonic domain. In the recent years new Fluid-Structure-Interaction (FSI) methods by means of coupled CFD and FE calculations have shown more accurate results in that Mach number domain. Within a common project of the Airbus Company and the German Aerospace Center (DLR) the described computational approach is used on the theoretical side. Experiments were performed in 2015 and 2017 to gain data for validation. The wind tunnel experiments were conducted by means of a forced motion experiment in a Mach number range of 0.7<M<1.2. The objective is to obtain the aerodynamic response to the panel's deformation. In order to simulate its first bending mode shape the all edge clamped panel is deflected by a hydraulic actuator. The structure is deflected sinusoidal over a wide range of amplitudes and frequencies. The wind tunnel's flow conditions are varied by means of the Mach number and the total pressure (Reynolds Number). Beside the measurement of the panel deformation by a stereo camera marker tracking system, the flow response is measured by high sensitive miniature pressure transducers.

KEYWORDS: *Forced Motion, Wind Tunnel Experiment, Transonic Domain, Aerodynamic Response, Aeroelastic stability*

NOMENCLATURE

Latin
Â - Amplitude
c_p - Pressure Coefficient
dz - Deformation in z direction
f - Frequency
l - Length of the panel
M - Mach Number
p - Pressure
q - Dynamic Pressure
Re - Reynolds Number
w - Width of the panel
x - x-Coordinate
y - y-Coordinate
z - z-Coordinate

Abreviations
CFD - Computational Fluid Dynamics
DNW - Dutch German Wind Tunnels
FE - Finite Elements
FSI - Fluid Structure Interaction
MBC - Mechanical Boundary Condition
RANS - Reynolds-Averaged Navier-Stokes
TWG - Transonic Wind Tunnel Göttingen

Greek
α - Panel Angle
δ - Boundary Layer thickness
φ - Phase Angle

Subscripts
0 - Total Value
∞ - Free Flow Condition
LE - Leading Edge
TE- Trailing Edge

1 INTRODUCTION

In the mid 1940's self-excited oscillations of skin panels of the first rockets was observed as a risk for the structural strength [1]. Accordingly, thorough investigation on the aeroelastic stability of plates and shells followed in the 1960's and 1970's both experimental and theoretical [2, 3, 4]. Experimental studies show that panels with clamped mechanical boundary conditions for all four edges are subjected to dynamic instabilities for supercritical Mach numbers. It was found that the non-dimensional critical dynamic pressure is strongly decreased in case of low supersonic Mach numbers. Further, an increase of the aerodynamic damping caused by the boundary layer of the fluid was observed. This second effect diminishes again the first one [5, 6] (see Fig. 1). Viscous flow was included in the theoretical investigation of the aeroelastic stability of panel structures. Linearized potential flow aerodynamics with an explicit definition of a non-uniform mean flow [7, 8] or an one-seventh power law for the flow velocity in a turbulent boundary layer was used [9, 10]. Later, the viscous flow was considered by using Reynolds-averaged Navier-Stokes equations [11, 12, 13]. Fig. 1 shows results of an exemplary two-dimensional flat plate simply supported at the leading edge and the trailing edge (adapted from [13]). With regards to the displayed Saturn V launch trajectory [14] the low supersonic domain is most critical. Depending on whether a non-viscous or a viscous calculation is done the critical dynamic pressure is exceeded and instabilities occur. Fig. 1 illustrates two different types of flutter concerning the same panel, which may appear based on the mentioned calculations. The flutter frequency is plotted against the Mach number. In the low supersonic domain so-called single-mode flutter appears which is dominated by the panel's first bending mode shape. For increased Mach numbers coupled-mode flutter emerges, which is a results of the first two bending mode shapes.

Hitherto performed experiments were focused on the determination of the critical dynamic pressure [5, 6, 15] for a wide range of Mach numbers and dynamic pressures for numerous parameters of panel geometry and material. In opposite to those experiments the approach of the test setup described in the report at hand is based on an actuated panel structure below the critical dynamic pressure. The panel structure is forced to take the mentioned mode shape (Fig. 2). The aerodynamic response is investigated by means of account of complex amplitudes of the measured pressure on the structure's surface. The overall goal is the determination of generalized aerodynamic forces and the analysis of the aeroelastic stability based on small perturbation theory in the frequency domain. It allows further, with regards to single-mode flutter, the investigation of the physical mechanism of negative aerodynamic damping by applying the energy method because the lowest eigenmode is weakly influenced by aerodynamic coupling effects (Fig. 1). This paper shows experimental results of two test campaigns performed at the DLR in the Transonic Wind Tunnel Göttingen (DNW-TWG) concerning the first flutter-mode-shape. The tests were conducted within a Mach number range of 0.7<M<1.2, a range of reduced frequencies of 0.0Hz<f<60Hz as well as several Reynolds numbers and deflection amplitudes. The description of the used test setup and the applied measurement techniques for deformation and pressure is followed by a presentation of the results by means of the measured aerodynamic response. The influence of the aforementioned parameters is illustrated.

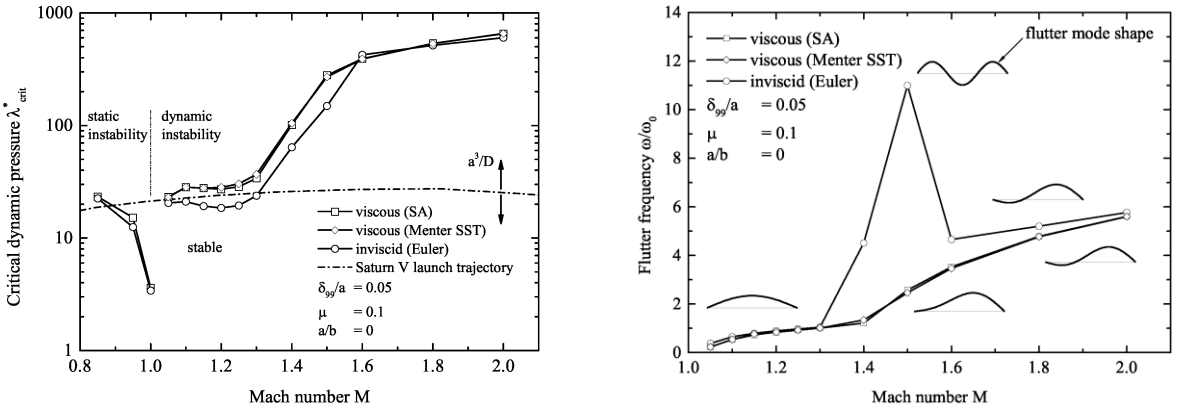

Fig 1: Numerical Results of a 2D panel [15]. Left: Aeroelastic stability boundary. Right: Flutter frequencies and emerging flutter shapes.

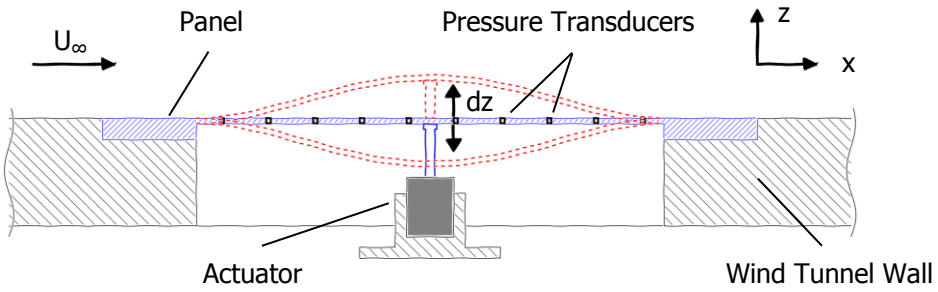

Figure 2: Test setup sketch.

2 EXPRIMENTAL REALISATION

For the investigation of the aerodynamic stability of panels a new test setup was designed and manufactured at DLR for the use in the DNW-TWG. Beside the wide range of flow conditions provided by the wind tunnel the test rig allows the application of various panel structures concerning geometry and materials. The test structure, which is chosen for the test campaigns presented in this report, is a flat rectangular plate, which is embedded in a frame structure (Fig. 3). First the test structure has to be mounted to the so-called Inner Frame (Fig. 3, left) which in return has to be applied into the Outer Frame (Fig. 3, right). The result is a 1m by 1m surface, which is to be connected to a as large as that slot in the wind tunnel wall. The applied Setup is accordingly a part of the wind tunnel wall with a panel, which has one surface exposed to the wind tunnel flow and one surface averted to the flow. The two-frame-design is a result of the intended modularity of the whole setup. The Inner Frame can be rotated α=90° to allow investigations for another length-to-width ratio of the test structure. This feature is not yet used in the performed tests.

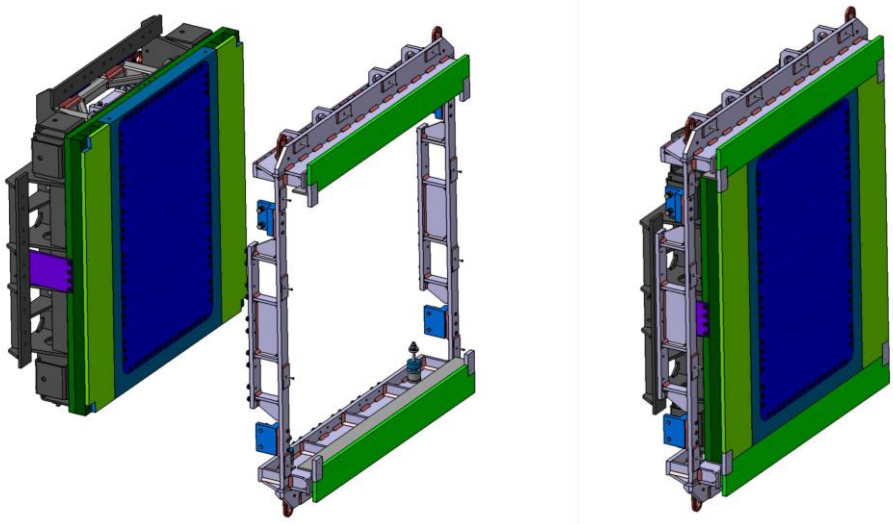

Figure 3: Test Setup. Left: The Inner Frame carries the panel structure. The Outer Frame connection the Inner Frame to the wind tunnel wall. Right: The flow facing part of the setup contains the panel (blue) and four wall plates of the two frames (green).

The used panel has a length-to-width ratio of $l/w = 500mm/875mm$ and is restrained with clamped mechanical boundary conditions (MBC's) for all four edges. The panel is milled from a single block of isentropic material whose length and width dimensions exceed the dimensions of the panel. So, an integrated thick framework at all four edges shall ensure the intended clamped MBC's (Fig. 3, Fig. 4). In order to deflect the panel surface a linear hydraulic actuator is applied on the wind averted side of the panel. The actuator applied at the panel center (x_{Cen}=0.5l, y_{Cen}=0.5w) shall meet the first bending mode of the panel. By performing a forced motion experiment that way the structural parameters of

the panel can be neglected. Though, information about the resulting forced shape is needed. The focus can be drawn on the aerodynamic response. The panel is equipped with various measurement techniques. Especially the measurement of pressure, by means of pressure transducers, and the measurement of the panel deflection (in z direction), by means of optical measurement, is essential. The aeroelastic system may be described by the deformation of the structure and the aerodynamic response by means of the surface pressure. For getting information of the entire surface of the panel both kinds of sensors are arranged in several intersections in x-direction as well as in y-direction (Fig. 4). In order to obtain an accurate measurement of the acting pressure 108 high sensitive unsteady pressure transducers are applied. Those transducers work on the principle of reference pressure and at a measurement range of 5 PSI. The deformation is measured by a stereo camera based marker tracking system. White markers are applied on the structure's dark surface. Two cameras, mounted outside the wind tunnel, track those markers simultaneously at 350 fps. Based on the two recorded sets of 2D data the 3D coordinates are calculated. The later on presented results are related to the intersection S_{p4} in case of the pressure transducers and S_{z5} in case of the deformation markers (Fig. 4). A more detailed survey on the test rig design and its instrumentation is available in Lübker et al. [17].

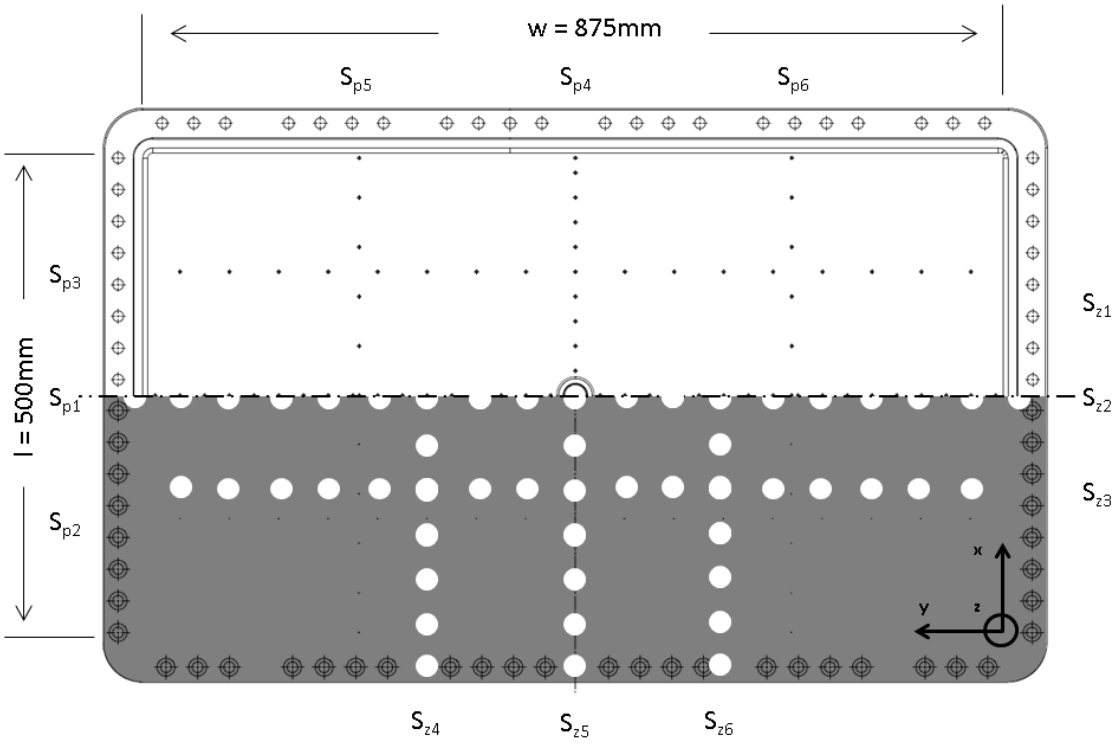

Figure 4: Flow averted side (upper half) and flow faced side (lower half) of the panel. The upper part shows the arrangement of the pressure transducers (S_{p1}-S_{p6}). The lower part shows the markers, which are tracked by the cameras (S_{z1}-S_{z6}). The massive framing, which exhibits a hole-pattern, around the panel is recognizable as well as the connection cone for the mode-shape-one-excitation in the panel's center.

The DNW-TWG is a closed return type wind tunnel, which is able to provide a large range of flow conditions. The experiments are focused on Mach numbers of $0.7<M<1.2$. The range of total pressure of $35kPa<p_0<135kPa$ enables the variation of the Reynolds number in between $2.5E+6<Re<7.5E+6$ (with reference length l). The applied actuators allow a maximum excitation amplitude of $\hat{A}_{MAX}$= 1.8mm. The excitation frequency can be increased up to f_{MAX}=60Hz at maximum amplitude. The results presented in the next chapter are obtained during two different test campaigns. During the first campaign the Reynolds number was kept constant. Beside the variation of the Mach number and the excitation frequency the amplitude was varied. The focus of the second campaign was drawn on the variation of the Reynolds number. Further, the reproducibility regarding the former campaign was verified.

Table 1: Test procedure

Campaign no.	1	2		
Re [E+6]	Re_1 = 2.5	Re_1 = 2.5	Re_2 = 5.0	Re_3 = 7.5
Â [mm]	$\hat{A}_1$ = 0.6			
	$\hat{A}_2$ = 1.2			
	$\hat{A}_3$ = 1.8	$\hat{A}_3$ = 1.8	$\hat{A}_3$ = 1.8	$\hat{A}_3$ = 1.8

3 RESULTS

3.1 Forced Shape

Foundation for following study of the aerodynamic response is accurate information on the forced structure shape. The intended deflection shape is equal to a flat plate's first bending mode shape. This shape is to be expected being one potential flutter shape. The quality of the carried out shape shall be discussed briefly. Examples for different Mach numbers at a low excitation frequency are shown in Fig. 5. The black dashed curve illustrates the intended design shape to illustrate the realized contour accuracy. The deflection is depicted along the panel's downstream center line (Fig. 4: Intersection S_{z5}). The right hand figure shows the phase shifts for the measured markers, which are referred to the actuators excitation. With exception of inaccuracies at x=0.9l the whole structure is oscillating without noteworthy phase differences.

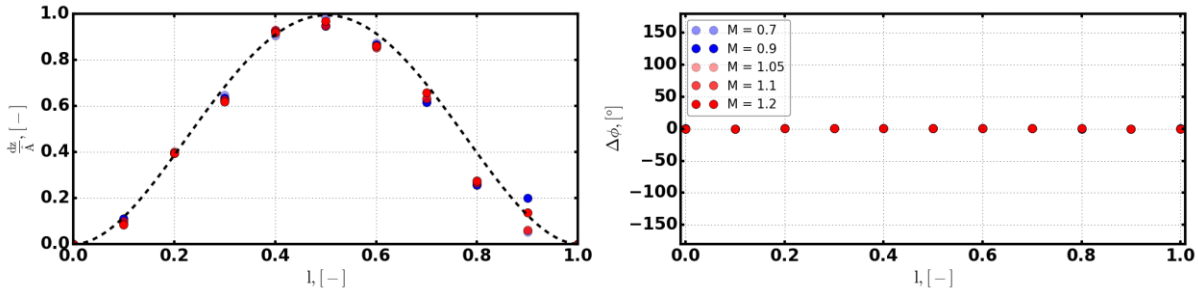

Figure 5: Amplitude (abs) and phase shift (related to the structure's excitation point at the centre) at low excitation frequency (f=1Hz, Re=2.5E+6).

3.2 Pressure Coefficient Response

This report is concentrating on the different influences on the pressure (coefficient) behavior. The main share is dedicated to the investigation of the influence of Mach number and excitation frequency. Besides that attention is drawn to the parameters Reynolds number and excitation amplitude. The reproducibility of the results is verified as well. Subsonic cases and supersonic cases will be illustrated. The results along the panel's center intersection in stream-wise direction are presented (see $S_{p,4}$ in Fig. 4). The pressure coefficient is normalized by its particular deflection amplitude. The most illustrations are done by means of four associated diagrams. On the one hand the measured complex values are broken into the absolute amplitude and the belonging phase shift. The phase shift is the resulting phase related to the structures oscillation phase, which identic to the actuator's movement. On the other hand the oscillations are illustrated by means of real part and imaginary part.

Before analyzing the influence of the different parameters a reference example for low subsonic flow conditions at a low excitation frequency shall be discussed (Fig. 5). Symmetry for the panel's half-length can be recognized. Three oscillating domains are illustrated which are separated by zero points at about $x_{Abs,1}$=0.2l and $x_{Abs,2}$=0.8l. The inflexion points of the deformed structure are located here. The phase distribution reveals that the two domains at the leading edge and at the trailing edge oscillate inversely phased compared to the center domain. Starting at the leading edge the phase

shift is constant at Δφ=0°. At the position of the deflected structure's first inflexion point a jump to Δφ=180° appears, which means an oscillation opposition. At the second inflexion point another jump appears and the phase is shifted back to Δφ=0° or Δφ=360° respectively. The same behavior must be distinguishable by regarding real- and imaginary part. The real part shows very clearly the zero points and the three different domains of the oscillation. By comparison it appears that the imaginary part is small, which means a low influence on the oscillation. In case of positive absolute values the phase is Δφ=0° and in case of negative absolute values the phase is Δφ=180°. The strongest impact of the imaginary part is at about $x_{Imag,1}$=0.15l and $x_{Imag,2}$=0.7l. In the phase plot the largest deviations from Δφ=0° and Δφ=180° occur here

Excitation Amplitude: With regards to the numerical activities and to the quality of the measurements it is important to get information on the dependency between the deflection amplitude and the measured pressure response. The tested amplitudes ($\hat{A}_1$, $\hat{A}_2$, $\hat{A}_3$) are chosen due to numerical studies and boundary conditions based on the structure's mechanical strength. Exemplary results of the pressure coefficient c_p normalized by the particular deflection amplitude are illustrated in Fig. 6. The agreement for all cases is satisfactory for all four plots. Small deviations are recognizable only for the imaginary part. However, the results are still very close to each other. Compared to the real part the imaginary part is very small. An increasing inaccuracy in the measurement may cause the deviations. Due to the normalization of the measurements by the excitation amplitude the results show a linear dependency of the pressure on the structure's deformation.

Reproducibility of Results: The first measurement campaign was done in the end of 2015. The second one followed in the beginning of 2017. A quality feature for an experiment is the reproducibility of results. Fig. 6 displays in addition to results of the first campaign results measured in 2017 at excitation amplitude A_3. The comparison of the 2015 results and the 2017 results shows an excellent reproducibility. The plot of the imaginary part shows again slight deviations.

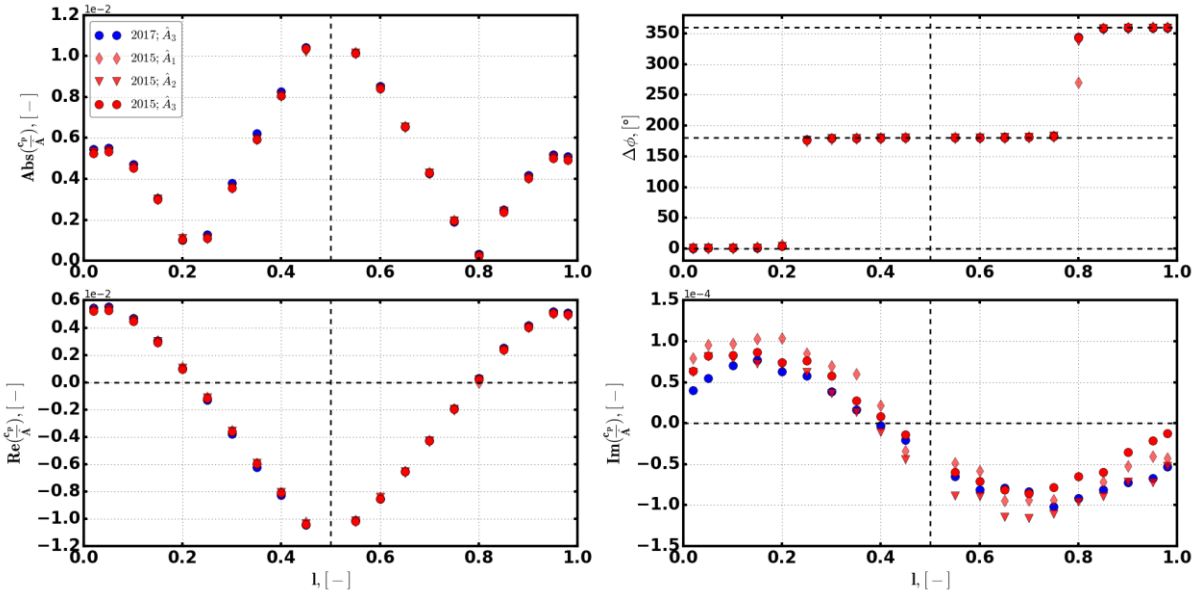

Figure 6: Dependency on excitation amplitude & reproducibility of results (M=0.7, f=1.0Hz, Re=2.5E+6).

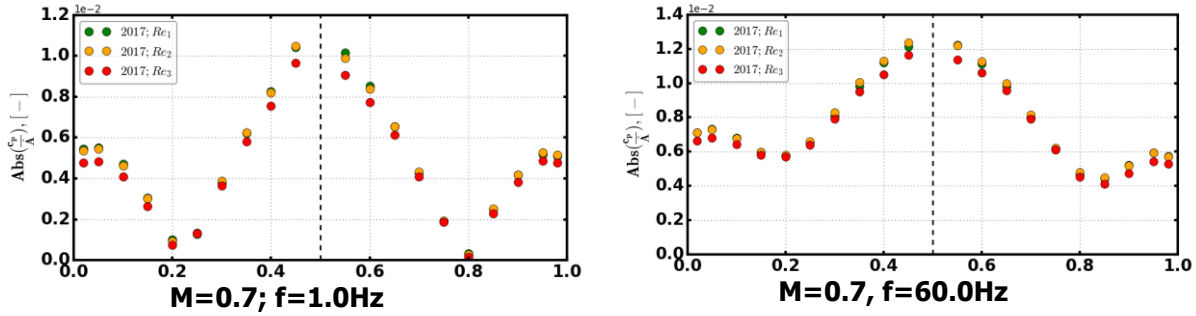

M=0.7; f=1.0Hz **M=0.7, f=60.0Hz**

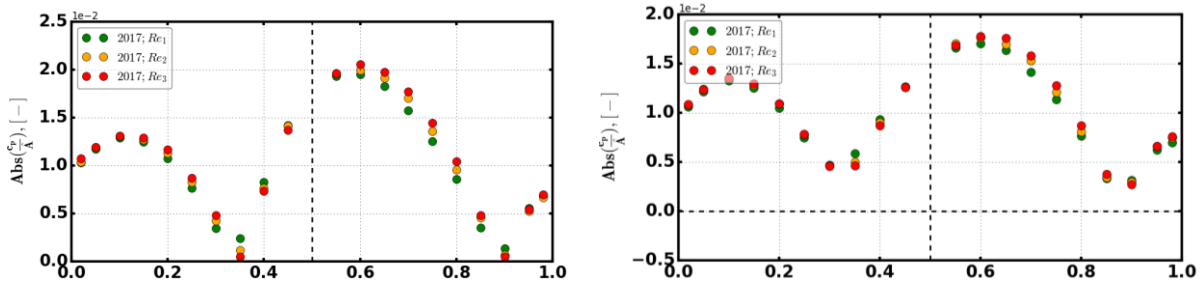

M=1.1; f=1.0Hz **M=1.1, f=60.0Hz**

Figure 7: Dependency on Reynolds number.

Reynolds Number Dependency: Three different Reynolds numbers are investigated (Re_2=2Re_1; Re_3=3Re_1; Fig. 7). The comparison shows a very slight influence on the pressure distribution. Although the impact is low, in case of Re_3 a decrease of the pressure amplitude appears in the subsonic domain. In case of high subsonic flow (M≥0.9) and supersonic flow conditions the high Reynolds number leads to increasing pressure amplitudes. The phase angle is not depending on the Re-number.

Mach Number Dependency: The already presented test conditions are at subsonic Mach number and for a low excitation frequency. The increase of Mach number at low excitation frequency in the subsonic domain leads to an increase in pressure amplitude as Fig. 8 reveals. The location of the stationary zero points and the turning points is not effected. Due to the even increase of real part and imaginary part the phase along the panel's length is unaffected. By exceeding of the critical flow conditions different phenomena occur. The Amplitude is strongly increased for a low supercritical flow of M=1.05 and a shift of the zero points is shown in stream-wise direction. Related to the panel's half-length the symmetry becomes asymmetric accordingly. The domain at the leading edge gains more intensity in spatial extend and in amplitude. In return the trailing edge domain is diminished.
The shift of the zero points is recognizable by regarding the amplitude and the phase shift by means of a shift of the changing positions from Δφ=0° to Δφ=180° crossing and back. With further increase of the Mach number the absolute value of the amplitude and its real part is decreasing more and more. The shift of the zero points is continuing. The decrease in amplitude and a down-stream shift of the turning points occur for the imaginary part as well. At least for M=1.05 and M=1.1. The imaginary part plot values for the third supersonic case are indistinct.

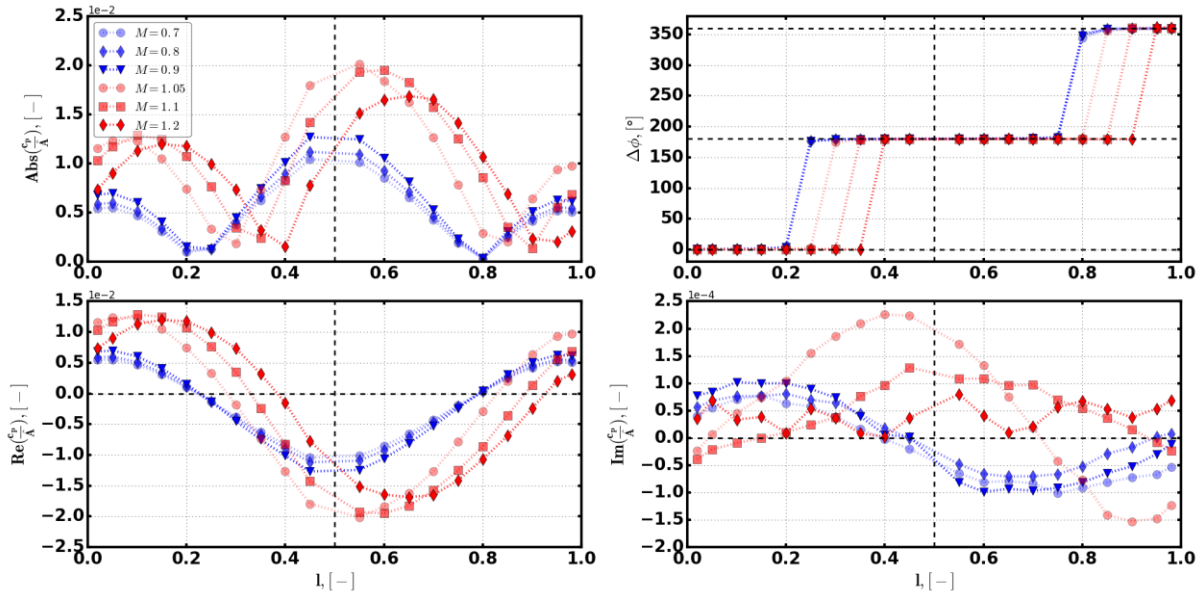

Figure 8: Influence of Mach number at low excitation frequencies (f=1Hz, Re=2.5E+6).

Fig. 9 illustrates the Mach number influence in case of a high excitation frequency (f=60Hz). Just as observed for the low frequency example the amplitude increases by increasing the subsonic Mach number. The Influence in the vicinity of the leading edge is much stronger than at the trailing edge. The change of the real part and the Imaginary part proves that. The real part is of the same magnitude for low frequencies and for high frequencies. In contrast to the former example the imaginary part is increased by a factor of about two orders of magnitude compared to the low excitation frequency. This has a very strong impact on the phase shift. The hitherto observed stepwise characteristic with phase angles at Δφ=180° or at Δφ=0° changes to a continuous increase along the panel length. The dependency in the subsonic domain on the Mach number is still small. For supersonic flow conditions at a high frequency the downstream shift of the Δφ=180° domain continuous. But in contrast to subsonic conditions the increase of the supersonic Mach number continuous the increase of the amplitude. Only the imaginary part starts with high amplitudes and is decreasing for increasing Mach numbers. The resulting phase shift shows the same continuous increase as detected at subsonic conditions. The higher the Mach number rises the more the characteristic of the low frequency domain dominates, regarding the sudden changes from in-phase to out-of-phase conditions.

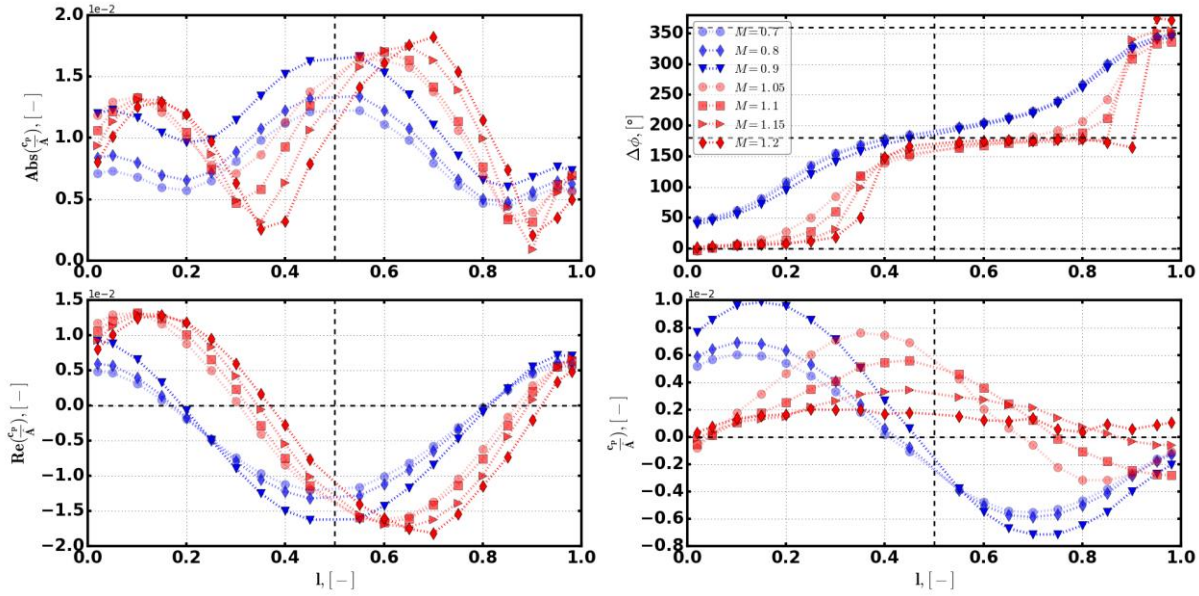

Figure 9: Influence of Mach number at high excitation frequencies (f=60Hz, Re=2.5E+6).

Frequency Dependency: The hitherto illustrated examples (Fig. 8; Fig. 9.) gave first impressions of the influence of the excitation frequency. First the subsonic case will be discussed in detail (Fig. 10). An increase of the frequency leads here to an increase of the amplitude. The stationary zero points at x_1=0.2l and x_2=0.8l vanish. This is caused by comparatively strong increase of the imaginary part. The result is a change of the entire phase shift characteristic. At f=1Hz the phase shift is observed to be φ=0° or φ=180°. Starting at φ=0° a jump happens to φ=180° and another step followed to φ=360° (back to φ=0°). The increase of frequency causes a phase shift at the leading edge (x_{LE}=0) up to φ=50°. The curve behavior changes from two distinct levels to an s-shaped curve, which approaches more and more a line with a constant inclination from φ_{LE}>50° to φ_{TE}=360°. The gradually rise of the imaginary part means standing wave characteristics for low frequencies with co-oscillating and counter-oscillating domains separated at the structure's inflexion points. Increasing frequencies entail a bit by bit transformation of those wave characteristic. The standing wave becomes a traveling wave. The development of the pressure distribution at low supersonic flow conditions (M=1.1) is presented in Fig. 11. The influence of the frequency on the pressure coefficient's amplitude is converse to the observations done at subsonic conditions. An increase in the Mach number means a decrease in the pressure coefficients amplitude. The same applies to the real part but does not for the imaginary part. Here an increase occurs as well as at subsonic conditions. A vanishing of the stationary zero points and the conversion to traveling wave characteristics occurs accordingly. This influence is less strong as detected for subsonic conditions. For the range of tested frequencies the phase at the leading edge is almost not shifted from about zero to higher degrees.

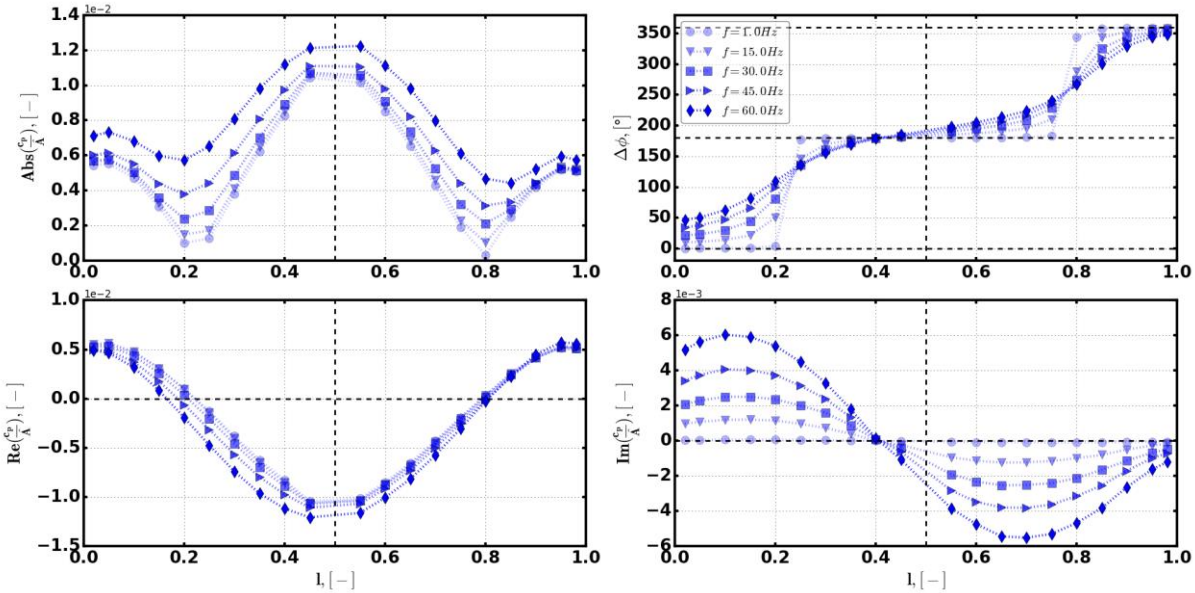

Figure 10: Influence of excitation frequency at subsonic flow conditions (M=0.7).

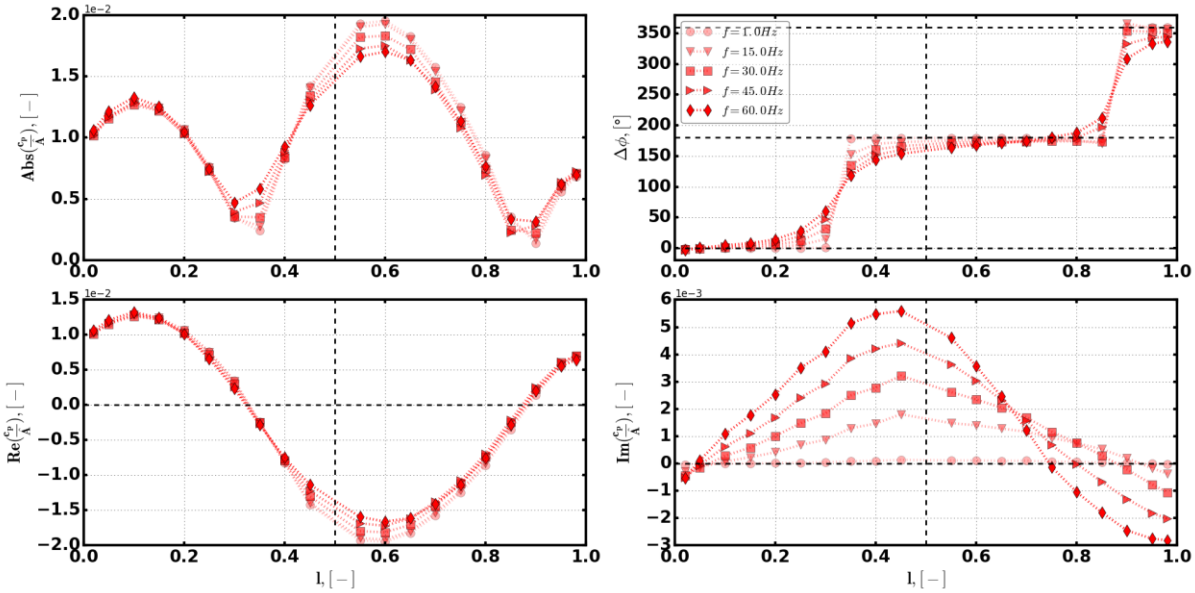

Figure 11: Influence of excitation frequency at supersonic flow conditions (M=1.1).

4 SUMMARY / OUTLOOK

4.1 Influence of Testparameters

In the tested range of deflection the dependency of the pressure response on the **deflection amplitude** is linear. The influence of the **Reynolds number** is low. In the subsonic domain an increase leads to a decrease of the pressure amplitude. From M=0.9 the high Reynolds numbers cause low amplitudes. A variation in a wider range could lead to more distinct results. The **Mach number** has a strong influence on the pressure response. At subsonic flow conditions a rise of the Mach number comes along with a rise of the pressure amplitude. The qualitative characteristics of the pressure distribution are not changed. No change of the phase shift occurs. At supersonic flow conditions an increase of the Mach number means an increasing shift of the φ=180° domain in down-stream direction. Further effects depend on the excitation frequency. At low frequencies a sudden increase of the amplitude occurs by exceeding the critical flow conditions. Particularly concerning the imaginary part. Further increases cause a drop of the amplitude. At high frequencies the amplitude is

continuously rising with increased Mach number. The distinct traveling wave, which was observed at subsonic flow conditions, loses its peculiarity. Not less influencing than the Mach number is the **excitation frequency**. Beside a decreasing and increasing impact on the pressure amplitude (depending on M), the frequency changes the characteristic of the transfer function of pressure response and deflection. An increasing frequency causes the conversion of a standing wave at low frequencies into a traveling wave at high frequencies.

4.2 Next Steps

Another test campaign with focus on the second bending mode-shape was performed 2017. To complete the needed data set for continue investigating the aeroelastic stability flat panels those data has to be analyzed. First preliminary comparisons of test results and numerical results were done for the 2015 test campaign. The work will be continued with the full set of required data including the followed two test campaigns. Another goal based the on the experiments is to obtain energy, which is transferred between the structure and the fluid by means of the structures movement and the pressure acting on the surface of the structure. The study will give information on domains in which energy is transferred in the structure, which leads to a diminishing of the damping.

REFERENCES

1. Garrick, I. E.; 1981; "Historical Development on Aircraft Flutter"; *Journal of Aircraft*; Vol. 18; No.11; pp. 897-912
2. Dowell, E. H.; 1975; "Aeroelasticity of Plates and Shells"; *Noordhoff International*; Leyden; The Netherlands; pp.139
3. Dowell, E. H.; 2010; "Panel Flutter, Encycl. of Aerospace Engineering"; *John Wiley & Sons Ltd*
4. Johns, D. J.; 1965; "A Survey on Panel Flutter"; *AGARD Advisory Rept. 1*
5. Muhlstein, L., Gaspers, P. A., Riddle, D.W.; 1968; "An experimental study of the influence of the turbulent boundary layer on panel flutter"; *NASA Technical Note*; D-4486
6. Gaspers, P. A, Muhlstein, L., Petroff, D.N.; 1970; "Further experimental results on the influence of the turbulent boundary layer on panel flutter"; *NASA Technical Note*; D-5798
7. Fung, Y. C.; 1963; "Some Recent Contributions to Panel Flutter Research"; *AIAA Journal*; Vol.1; No. 4; pp. 898-909
8. Zeydel, E. F. E.; 1965; "Study of the Pressure Distribution on Oscillating Panels in Low Supersonic Flow with Turbulent Boundary Layer"; http://hdl.handle.net/1853/49798; Engineering Experiment Station; Project no. B-208; Georgia Institute of Technology
9. Dowell, E. H.; 1970; "Generalized Aerodynamic Forces on a Flexible Plate Undergoing Transient Motion in a Shear Flow with an Application to Panel Flutter"; *AIAA 8th Aerospace Sciences Meeting*
10. Dowell, E. H.; 1973; "Aerodynamic Boundary Layer Effects on Flutter and Damping of Plates"; *Journal of Aircraft*; Vol. 10; No. 12; pp. 734-738
11. Hashimoto, A.; 2009; "Effects on Turbulent Boundary Layer on Panel Flutter"; *AIAA Journal*; Vol.47; No.12; pp. 2785-2791
12. Shishaeva, A., Vedeneev, V. V., Aksenov, A.; 2015; "Nonlinear single-mode and multi-mode panel flutter oscillations at low supersonic speeds"; *Journal of Fluids and Structure*; Vol. 56, pp. 205-223
13. Alder, M.; 2015; "Development and Validation of a Partitioned Fluid-Structure Solver for Transonic Panel Flutter with Focus on Boundary Layer Effects"; *AIAA Journal*; Vol. 53; No. 12; pp. 3509-3521
14. Perkins, T. M.; 1968; "Flutter Test of an Array of Full-Scale Panels from the Saturn S-IVB Stage at Transonic Mach numbers"; *AD827913*
15. Vedeneev, V. V., Guvernyuk, S. V., Zubkov, A. F., Kolotnikov, M. E.; 2009; "Experimental observation of single-mode panel flutter in a supersonic gas flow"; *Doklady Physics*; Vol. 54; No. 8; pp. 389-391
16. Muhlstein, L.; 1966; "A FORCED VIBRATION TECHNIQUE FOR INVESTIGATION OF PANEL FLUTTER", *AIAA Paper*; No. 66-769; AIAA Aerodynamic Testing Conference
17. Lübker, J., Alder, M., Fink, H.; 2016; "DESIGN AND INITIAL RUN OF A NEW TEST SETUP FOR INVESTIGATIONS ON THE AEROELASTIC STABILITY OF PANELS IN THE TRANSONIC MACH DOMAIN"; *ECSSMET 2016;* Toulouse; September; 27.-30